On the rejection of vibrations in Adaptive Optics Systems

Riccardo Muradore[a], Lorenzo Pettazzi[b], Enrico Fedrigo[b] and Richard Clare[b]

[a]University of Verona, Department of Computer Science, Italy
[b]European Southern Observatory (ESO), Karl-Schwarzschild-Strasse. 2, Garching, Germany

ABSTRACT

In modern adaptive optics systems, lightly damped sinusoidal oscillations resulting from telescope structural vibrations have a significant deleterious impact on the quality of the image collected at the detector plane. Such oscillations are often at frequencies beyond the bandwidth of the wave-front controller that therefore is either incapable of rejecting them or might even amplify their detrimental impact on the overall AO performance. A technique for the rejection of periodic disturbances acting at the output of unknown plants, which has been recently presented in literature, has been adapted to the problem of rejecting vibrations in AO loops. The proposed methodology aims at estimating phase and amplitude of the harmonic disturbance together with the response of the unknown plant at the frequency of vibration. On the basis of such estimates, a control signal is generated to cancel out the periodic perturbation. Additionally, the algorithm can be easily extended to cope with unexpected time variations of the vibrations frequency by adding a frequency tracking module based either on a simple PLL architecture or on a classical extended Kalman filter. Oversampling can be also easily introduced to efficiently correct for vibrations approaching the sampling frequency. The approach presented in this contribution is compared against a different algorithm for vibration rejection available in literature, in order to identify drawbacks and advantages. Finally, the performance of the proposed vibration cancellation technique has been tested in realistic scenarios defined exploiting tip/tilt measurements from MACAO and NACO

Keywords: Adaptive Optics, Vibration rejection, Adaptive Control

1. INTRODUCTION

The effect of vibrations that could be present in various places in the telescope's optical train is a topic that has generated growing interest over the past years. It affected the NACO (NAOS/CONICA) system at the ESO Paranal Observatory: vibrations have been identified as one of the main reasons NAOS could not perform as predicted and tested in the laboratory (see[1]). Another study[2] identified vibrations as one of the causes preventing fringe tracking in the ESO VLT Interferometer. Several measures have been taken then to prevent these lightly damped harmonic oscillations from being generated and propagated to the optical components, like damping or isolations of vibrations sources like fans, but not all vibrations could be suppressed in this way. In some cases the effect of vibrations can be observed on a wavefront sensor and a vibration rejection algorithm can be used to reduce their effect. Therefore this new component of the adaptive optics control loop has become an integral part of all the new instruments being designed since then.

In fact during the design of the GALACSI AO module[3] for MUSE[4] within the ESO Adaptive Optics Facility[5] the Analysis Report pointed out that the top performance of the highest Strehl mode, the so-called Narrow Field-of-View Mode (NFM), was severely hampered by the vibrations that are expected to be present on the telescope. The vibrations considered in the report were the ones observed on NACO[1] and are located primarily on tip and tilt at frequencies around 16-18 Hz and 48-55Hz. The report therefore mandated a research work to identify an algorithm and a strategy to remove those vibrations in order to bring GALACSI NFM back into specifications.

Over the past 30 years vibration cancellation (VC) algorithms have been developed to address similar issues in a variety of industrial applications ranging from noise reduction in airplane fuselages and train cars to vibration suppression in helicopter blades (see for example[6] and[7] for an overview and a comparison between several

Further author information: (Send correspondence to Riccardo Muradore, email: riccardo.muradore@univr.it, Telephone: (+39) 045 802 70 49)

approaches). In particular, in the recent past a renewed interest in the problem of rejecting vibrations propagating in astronomical telescopes has driven a considerable amount of research both in estimating the impact of vibrations on the closed loop image quality of AO systems (see for example[8]) and in devising algorithms for the mitigation of such detrimental perturbations (see for example[9,10] and[11,12]).

In this paper we report on the results of the work performed in order to identify, among the many algorithms developed in literature, the one that better allows the mitigation of the impact of vibrations on the existing and upcoming ESO AO systems.

2. PROBLEM STATEMENT

The present paper details the development of a vibration cancellation algorithm to be implemented in the Standard Platform for Adaptive optics Real Time Application (SPARTA see[13] for an overview) developed to steer the upcoming and currently-deployed ESO's Adaptive Optics systems.

The expected operational conditions and the requirements imposed by the implementation platform (i.e. SPARTA) define design constraints that in turn guided the choice of the approach proposed in this paper among the many others available in literature. In particular, the following design drivers were identified early in the development process:

- The VC algorithm shall feature a modular design in which the vibration cancellation functionality is encapsulated into a self-contained software module possibly to be executed in parallel to the existing AO controller. The benefit associated to this approach is twofold: on one side it allows deploying the algorithm on an existing AO system (either to improve the performance of the AO system itself or for on-sky validation of the VC algorithm) without requiring a complete re-commissioning of the entire wave-front controller. On the other hand it offers the possibility to better evaluate the performance of the algorithm independently of the target system.
- The VC algorithm shall be capable of coping with the (possibly) time-varying harmonic signals observed at the ESO Paranal observatory. Hence on-line estimation of both vibration amplitude and frequency shall be performed in order to correspondingly update the parameters of the VC algorithm during operation.
- The VC algorithm shall be able to work in a fairly large spectrum of conditions dictated by the different science cases (e.g. different sampling rates, switching of different measurement sources etc.) requiring the least possible direct operator's intervention.

The description of the algorithm designed in order to fulfill the requirements mentioned above is the subject of the next section.

3. ADAPTIVE CANCELLATION ALGORITHM

In literature there are several papers dealing with the rejection of vibrations or sinusoidal disturbances. In the present paper we tackle this problem by using the control technique known as adaptive control. Such well known and flexible approach is mandatory in the present context because, as mentioned in section 2 we don't want to assume any *a priori* knowledge on the plant and, more demanding, on the kinds of variation the vibrations are affected by.

Our approach is a slight modification of the algorithm proposed by Pigg and Bodson recently in a couple of papers[14,15] dealing, respectively, with the two following working conditions:

1. the frequency of vibration is fixed and known,
2. the frequency of vibration is unknown and has to be estimated.

Moving from the first to the second condition is not at all a trivial step. We will start in the following subsection to briefly recall the idea behind this approach, then the improvements required by the *unknown vibration frequency* case will be described. Finally our version of such algorithm that better fits the specific requirements in an AO system will be reported. It shall be highlighted that the proposed algorithm has a strong theoretical foundation that allows to (even though it is not reported here) prove stability in a rigorous way requiring minimum assumptions on the dynamics of the plant.

3.1 Unknown plant and known vibration frequency

The proposed methodology belongs to the family of active vibration control (AVC) applications. The algorithm consists of a two-step procedure:

1. online estimation of the frequency response of the plant at the vibration frequency and of the harmonic perturbation parameters,
2. update the control command to cancel/minimize the vibration.

The equations related to these two steps are reported below as *state equation* and *output equation*, respectively. These names come from the fact that the algorithm can be implemented in a non linear state-space representation.

The main advantage of this algorithm is that it works also when the plant is a time-varying system whereas the major drawback is that the vibration frequency must be known in advance. Even though the original algorithm assumes a basic feedback control configuration without reference signals and colored noise, in the simulation section it will be shown that this approach performs well also when time-varying signals are involved.

Assuming that the measurement takes the form:

$$y(t) = P(s)u(t) + v(t) \tag{1}$$

where $P(s)$ is the (BIBO linear) transfer function of the plant (unknown) and $v(t)$ is the vibration we have to reject by the control signal $u(t)$. The sinusoidal signal describing the vibration at frequency f_i can be written as

$$v(t) = \lambda_c \cos(2\pi f_i t) + \lambda_s \sin(2\pi f_i t) = w_i^T(t)\lambda \tag{2}$$

where

$$w_i(t) = \begin{bmatrix}\cos(2\pi f_i t) \\ \sin(2\pi f_i t)\end{bmatrix} \tag{3}$$

$$\lambda = \begin{bmatrix}\lambda_c \\ \lambda_s\end{bmatrix}. \tag{4}$$

A control signal of the form

$$u(t) = \theta_c \cos(2\pi f_i t) + \theta_s \sin(2\pi f_i t) = w_i^T(t)\theta \tag{5}$$

for the right θ can be used to cancel the vibration $v(t)$ in (1). This means that in steady state (with only the sinusoidal signal as input), the output of the plant is

$$y(t) = P(s)u(t) + v(t) = w_i^T(t)(G\theta^* + \lambda) \sim 0 \tag{6}$$

where θ^* is the adaptive parameter that the algorithm has to determine and G is a matrix containing the unknown real and imaginary parts of the plant's frequency response at f_i ($P(j2\pi f_i) = P_R + jP_I$), i.e.:

$$G = \begin{bmatrix}P_R & P_I \\ -P_I & P_R\end{bmatrix}. \tag{7}$$

State equation

Collecting in the state vector x the unknowns, i.e. $x := \begin{bmatrix} P_R & P_I & \lambda_c & \lambda_s \end{bmatrix}^T$, the equation (6) can be rewritten as

$$y(t) = W(t,\theta)^T x \tag{8}$$

where the time-varying regressor matrix takes the form

$$W(t,\theta) = \begin{bmatrix} \theta_c \cos(2\pi f_i t) + \theta_s \sin(2\pi f_i t) \\ \theta_s \cos(2\pi f_i t) - \theta_c \sin(2\pi f_i t) \\ \cos(2\pi f_i t) \\ \sin(2\pi f_i t) \end{bmatrix}. \tag{9}$$

By using a gradient algorithm for the minimization of the squared error $\varepsilon^2 = (W(t,\theta)^T x - y)^2$, we end up with the following non linear time-varying differential equation and its Euler discretization with sample time T_s:

continuous-time	discrete-time
$\dot{x}(t) = -g_x W(t,\theta)(W(t,\theta)^T x(t) - y(t))$	$x(t+1) = x(t) - g_x T_s W(t,\theta)(W(t,\theta)^T x(t) - y(t))$

(10)

where the adaptation parameter $g_x > 0$ is a tuning parameter. It is important to highlight that very limited prior knowledge of the plant dynamics is required to initialize the algorithm: the AVC will estimate the response of the unknown plant within few iterations. The only condition is that the first and the second component of $x(0)$ cannot be both equal to zero.

Since the discrete-time equations are parametrized in the sampling time T_s, the tuning parameter g_x should be almost the same even if the integration time (equal to T_s) of the NGS-WFS changes.

Output equation

When a new estimation of $x(t)$ is available, it is possible to compute a new estimation of θ as

$$\theta(t) = -\frac{1}{x_1^2 + x_2^2} \begin{bmatrix} x_1 x_3 - x_2 x_4 \\ x_1 x_4 + x_2 x_3 \end{bmatrix} \tag{11}$$

and the updated control command becomes

$$u(t) = w_i^T(t)\theta(t). \tag{12}$$

Remark Since the system may be affected by more than one vibration at the same time, as many AVC modules as vibrations have to be put in parallel to the controller of the AO loop.

3.2 Unknown plant and unknown vibration frequency

To cope with the unknown vibration frequency, an updated version of the previous algorithm is obtained by coupling the original AVC with a Magnitude/Phase locked loop (MPLL) estimator.[15] Alternative frequency tracking methodologies (e.g. Extended Kalman Filter) can be also considered for such purpose. The MPLL solution was however selected for its simplicity and for the lower required computational power. Let $m(t)\cos(\alpha(t))$ be a representation of a vibration with time-varying amplitude $m(t)$ and phase $\alpha(t)$. The MPLL has the following equations

continuous-time			discrete-time		
$\dot{m}(t)$	$=$	$2g_m \cos(\alpha(t))e(t)$	$m(t+1)$	$=$	$m(t) + 2g_m T_s \cos(\alpha(t))e(t)$
$\dot{\omega}(t)$	$=$	$-2g_\omega \sin(\alpha(t))e(t)$	$\omega(t+1)$	$=$	$\omega(t) - 2g_\omega T_s \sin(\alpha(t))e(t)$
$\dot{\alpha}(t)$	$=$	$\omega(t) - 2g_\alpha g_\omega \sin(\alpha(t))e(t)$	$\alpha(t+1)$	$=$	$\alpha(t) + T_s\omega(t) - 2g_\alpha g_\omega T_s \sin(\alpha(t))e(t)$

(13)

where $\omega(t)$ is the pulsation corresponding to the phase $\alpha(t)$, $e(t)$ is the MPLL feedback error

$$e(t) = y(t) - m(t)\cos(\alpha(t)). \tag{14}$$

and g_m, g_ω, g_α are again tuning parameters.

The value of $\alpha(t) = 2\pi f_i t$ is the input needed by the AVC in (9) to compute $W(t,\theta)$ and in (3) to compute $w_i(t)$. Since both the AVC and the MPLL estimate the amplitude of the vibration (the AVC implicitly in the last two components of state vector, the MPLL in the dynamic equation involving $m(t)$), the transients of the two dynamical systems are badly affected by this coupling. This is particularly true when the variation of the vibration parameters is fast and the signal-to-noise ratio is not so high as in common working conditions (e.g. faint star used to correct the atmosphere). For this reason we simplified the original formulation by removing the estimation of the amplitude within the MPLL: this means that the value of the amplitude needed within the MPLL is provided by the AVC equation. At the end the mathematical model of the vibration rejection module is given by:

continuous-time			discrete-time			
$\dot{x}(t)$	$=$	$-g_x W(t,\theta)(-e(t))$	$x(t+1)$	$=$	$x(t) - g_x T_s W(t,\theta)(-e(t))$	(15)
$\dot{\omega}(t)$	$=$	$-2g_\omega \sin(\alpha(t))e(t)$	$\omega(t+1)$	$=$	$\omega(t) - 2g_\omega T_s \sin(\alpha(t))e(t)$	
$\dot{\alpha}(t)$	$=$	$\omega(t) - 2g_\alpha g_\omega \sin(\alpha(t))e(t)$	$\alpha(t+1)$	$=$	$\alpha(t) + T_s\omega(t) - 2g_\alpha g_\omega T_s \sin(\alpha(t))e(t)$	

where

$$e(t) = y(t) - W(t,\theta)^T x(t) \tag{16}$$

is the error used both within the AVC and the "modified" MPLL (that is now more an PLL than a MPLL). In this way we have simplified the model (i.e. we save one parameter) and, at the same time, we have removed the principal source of instability in the AVC.

3.3 Comparison with Existing Adaptive Vibration Cancellation Algorithms

The AVC described in 3.1 and 3.2 is somehow reminiscent of the adaptive vibration cancellation algorithm proposed in[10] for stellar interferometry. Both algorithms have been developed to cope with the problem of filtering out a narrow band signal perturbing the output of a linear plant. Both vibration rejection modules consist of two subsystems, one performing the on-line estimation of the instantaneous amplitude and phase of the incoming perturbation signal and one tracking eventual frequency variations. The algorithm in[10] requires an approximate knowledge of the delay/lags in the plant in order to generate appropriate correction signals. Although this approach is in general robust also in the presence of fairly large uncertainties in the plant dynamics, it might not be capable to cope - without operators intervention - with the broad spectrum of conditions defined in section 2. On the other hand the AVC described in the present paper is derived without assuming any knowledge of the plant dynamics (which is estimated on-line) and therefore it is by design more robust to modifications of the operational conditions. An in-depth discussion on stability and robustness properties of the AVC can be found in[14] and.[15]

4. SIMULATION RESULTS

4.1 Adaptive Optics System

Figure 1 reports the block diagram of the typical AO system considered for performance evaluation. There are two AO loops: the loop using the measurement coming from the NGS WFS that is used to correct the tip/tilt mode and the vibrations, and the jitter loop necessary to make the LGS WFS working in its linear regime. Even though in the present block diagram only one jitter loop has been included, as many jitter loops as LGS WFSs might be present in the system. Vibrations are assumed to propagate consistently through both the NGS and LGS path. This implies that if the vibration is removed within the NGS loop, it will also disappear in the LGS loop.

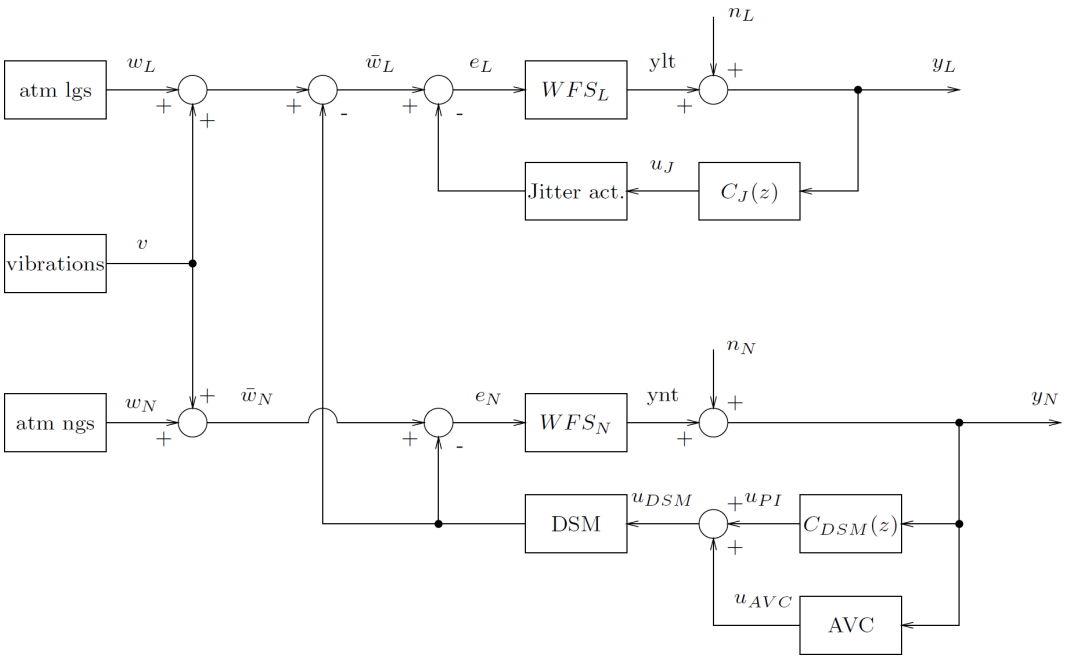

Figure 1. AO block diagram

The controllers are standard PID controllers tuned in order to have sufficient stability margins. The AVC is implemented in a separate module in parallel to the DSM controller. As already mentioned in section 2 the proposed architecture ensures that the AVC is independent of the DSM controller: the same AVC can be used for whatever controller is implemented and can be switched off and on without endangering the closed loop stability of the overall AO system.

In Figure 2 the Bode diagram of the DSM transfer function considered in the simulation model is displayed.

4.2 Definition of perturbation signal

The performance of the AVC is evaluated considering two test cases each one assuming a different disturbance signal representative of the typical perturbations affecting the performance of the existing AO systems deployed at the Paranal observatory.

In the first test case the theoretical atmospheric turbulence mapped into the tip/tilt modes displayed in Figure 3 is superimposed to vibrations signals extracted from closed loop slopes measurements performed by the NACO system. Structural vibrations can be conveniently represented as the output of second order systems which are characterized by vibration frequency and damping coefficient. Such parameters have been identified by processing the available closed loop NACO measurements according to the following procedure:

- Two different frequency regions are identified, one within and one beyond the NACO controller bandwidth. This allows to assess the performance of the vibration rejection algorithm in different conditions (for example in terms of SNR).
- The available 18 batches of measurement data sampled at 444 Hz have been scanned in order to find, within the abovementioned frequency regions, the vibrations with highest average power and thus having the largest impact on the image quality.
- Parameter estimation is performed in order to calculate frequency and damping coefficient of the worst-case vibrations defined in the previous step. To this end, a high-order auto-regressive model is fitted to the corresponding batch of closed loop NACO measurements by means of standard Yule-Walker method (see[16]). Then AR2 models corresponding to the high energy vibrations are factored out from the high order model and the vibration parameters are finally derived.

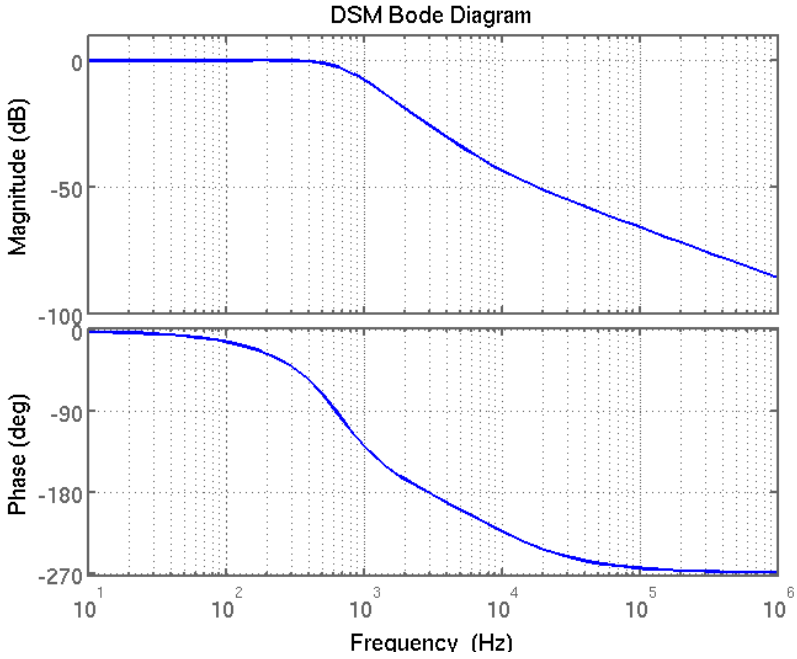

Figure 2. Bode diagram of the DSM-tip/tilt.

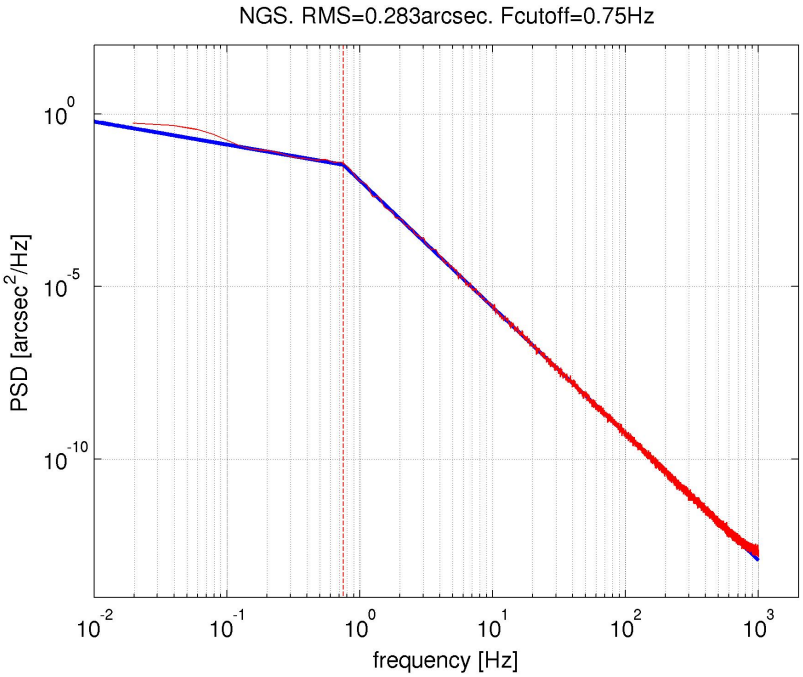

Figure 3. PSD of the incoming NGS atmosphere. (Blue line: theoretical spectrum, red line: PSD of numerical realization)

The technique briefly described above is demonstrated in Figure 4 and 5. The power spectrum of the batches of data including the worst-case vibrations is shown in Figure 4. In Figure 5 the PSD computed from raw data (red line), the PSD of the high order AR model (blue line) and the PSD of the AR2 model representing structural vibrations (green line) are plotted together. Vibration frequency and damping coefficients of the worst-case vibrations are finally listed in Table 1.

In the second case MACAO pseudo-open-loop data recorded during tracking of a calibration source are used in order to generate the perturbation signal driving the simulation model shown in Figure 1.

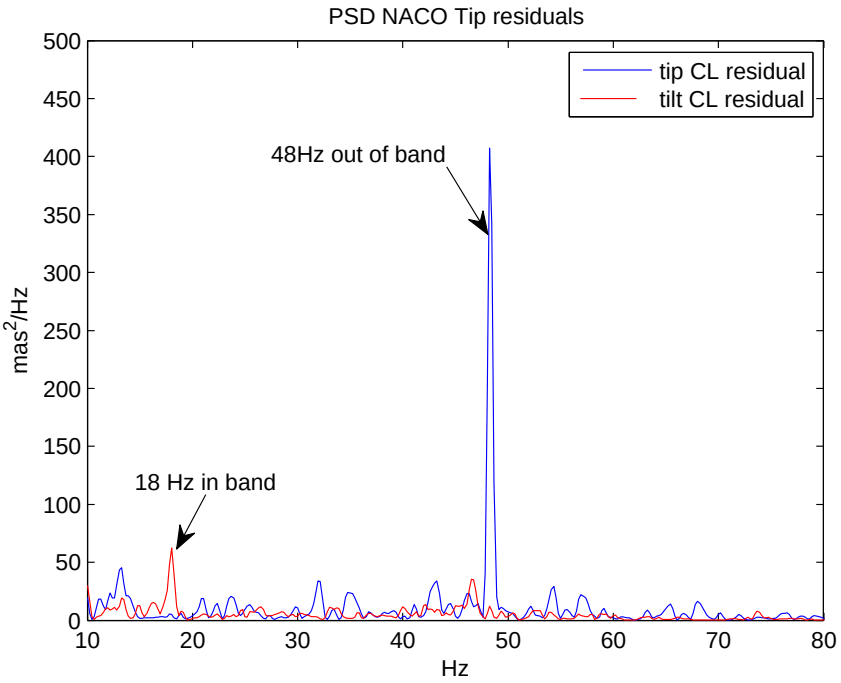

Figure 4. Power Spectral Density of NACO tip/tilt data.

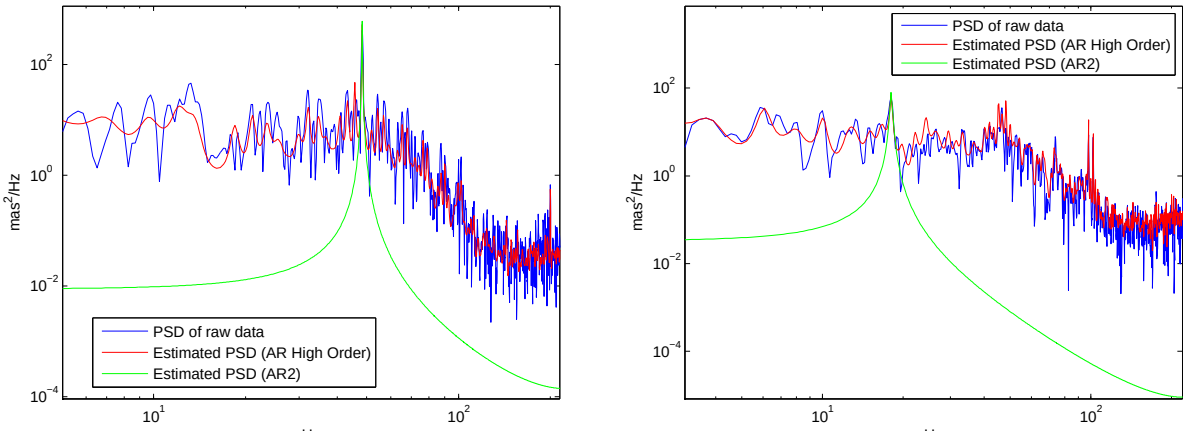

(a) AR2 estimation of 48Hz NACO tip vibration. (b) AR2 estimation of 18Hz NACO tilt vibration.

Figure 5. Characterization of NACO vibrations

4.3 Vibration Rejection

In order to evaluate the quality of the vibration rejection achieved by the AVC, two metrics have been used:

1. The first metric is the standard deviation of the residual, i.e. we compare the residual with and without the AVC. This metric is strongly related to the Strehl ratio and so to the final resolution of the images.

2. The reduction of the vibration peak (in dB) as seen in the PSD plot.

Vibration frequency	Damping ratio	FWHM
48Hz	0.001	0.15Hz
18Hz	0.008	0.48Hz

Table 1. Parameters of NACO vibrations.

The second metric is less accurate than the first one because the sharpness of the peak might depend on the algorithm used to compute the PSD which is in turn also affected by the kind of windowing and by the number of points used. In order to keep the presentation of the results consistent throughout the section, we always use the Welch method with Hanning windowing to compute the power spectral densities.

Figure 6 shows the results obtained using the AVC in the first test case assuming the control configuration of Figure 1. The simulation length is 250s with 2ms integration time. Compared with the case without the vibration rejection module, the RMS of the tip/tilt residual reduces from $15.2mas$ to $11mas$. This can be easily seen by comparing the cumulative PSD (top right plot) and the rejection of the vibration peaks at $18Hz$ and $48Hz$. It is worth remarking that the vibration at $48Hz$ is much more critical than the vibration at $18Hz$ because it is located close to the amplification range of the rejection transfer function. The rejection is on average larger than $20dB$. The AVC tuning is not at all problematic: here we have used the same parameters to reject the two vibrations using as initial conditions approximate values of the closed loop plant.

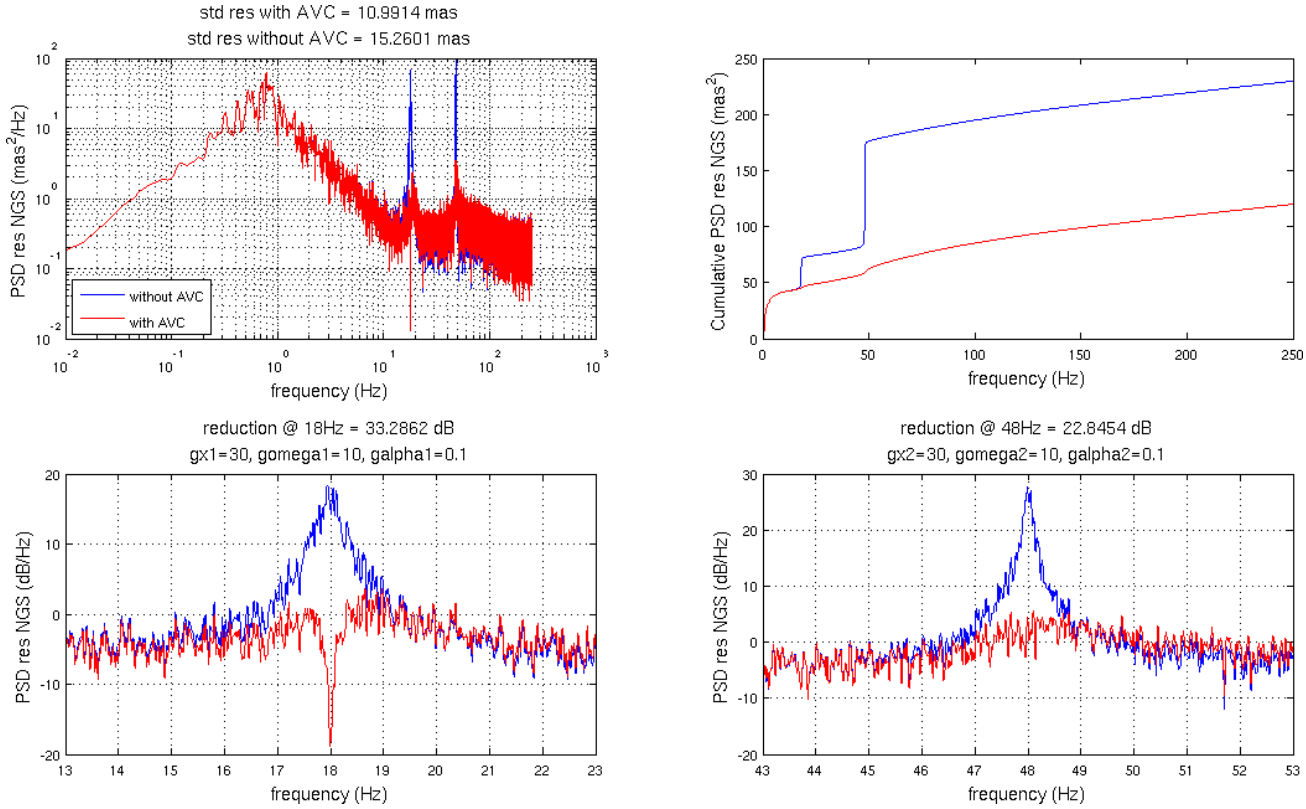

Figure 6. Experimental validation of the vibration rejection algorithm: test case 1.

The second test was performed using as input signal the POL data obtained from MACAO measurements. With respect to the previous setup, the sampling frequency of the control loop is $420Hz$ instead of $500Hz$. In Figure 7 two AVC modules are implemented correcting the vibrations around $48Hz$ and $97Hz$ respectively. The peaks are completely removed as can be easily seen from the PSDs and the cumulative PSDs in the Figure. It is also interesting to observe that the vibration frequency is quite stable ($\pm 0.1Hz$) whereas the amplitude has huge variations with fast dynamics. Nevertheless, the AVCs easily track the vibrations rejecting them completely.

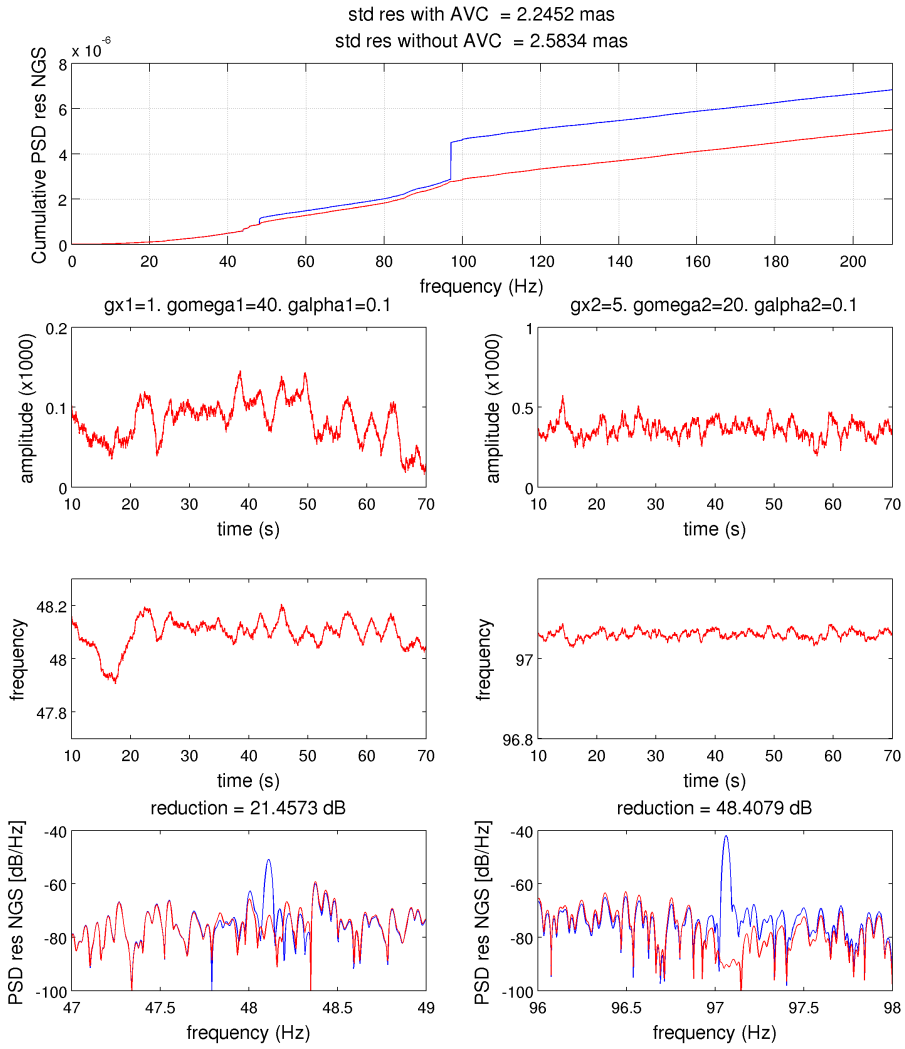

Figure 7. Experimental validation of the vibration rejection algorithm: test case 2.

4.4 Oversampling

The quality of the rejection of the vibration is related to the ratio between the vibration frequency and the sampling rate of the control loop. However, since the vibration can be easily written in mathematical term, it is possible to foresee the future corrections even when no new measurements are available. Let $y(t_k)$ be the last tip/tilt measurement received at $t_k = kT_s$, and N be the oversampling factor. Between two measurements it is possible to send to the DSM the "predicted" corrections at sample time $\frac{T_s}{N}$

$$u(k,h) = \begin{bmatrix} \cos(\alpha(k,h)) & \sin(\alpha(k,h)) \end{bmatrix} \hat{\theta}(k), \qquad h = 1, \ldots, N-1 \tag{17}$$

where

$$\alpha(k,h) = \alpha(k) + 2\pi \hat{f}_i(k) h \frac{T_s}{N} \tag{18}$$

with $\hat{f}_i(k)$ the estimation of the vibration frequency at time k. The value $\hat{\theta}(k)$ is the last prediction coming from the AVC using the last measurement available. This value is assumed frozen between two measurements.

The performance of the AVC with oversampling has been tested against NACO-like perturbations. However, in the test case selected (assuming vibrations at 18 and $48Hz$) the observed performance improvement is negligible because the AVC running at $0.5kHz$ is well enough to reduce the vibration peaks at the noise level. Advantages can be expected when the vibration frequency is close to the Nyquist frequency of the NGS loop (see for example[12]).

5. CONCLUSIONS

This paper details the development of an adaptive control system for the rejection of vibrations affecting the performance of adaptive optics systems. The algorithm proposed, which is an adaptation of the one presented in,[14,15] does not rely on the knowledge of the dynamics of the AO system and is therefore capable to cope with a broad spectrum of operational conditions requiring minimum operator's intervention. Additionally it lends itself quite naturally to a modular implementation which make it particularly suitable for being implemented in both existing and future ESO AO systems.

The performance of the vibration cancellation algorithm has been evaluated by means of numerical simulations carefully defined in order to reproduce the typical operational conditions to be expected at the Paranal observatory. The results of the performance assessment campaign has shown that high quality vibration cancellation can be achieved in all the scenarios analyzed.

As a final remark note that each AVC module is quite simple consisting of about 50 floating point operations and 2 sin/cos operations. In other words one AVC module is equivalent to a single 7x7 matrix-vector multiply operation and the 2 sin/cos calls have a similar cost, but can be removed by means of a look-up tables. This is clearly compatible with the computing power available in the CPUs of the SPARTA back-end system, where the algorithm will be implemented.

REFERENCES

[1] Y. Clenet, "NAOS Performance Report," tech. rep., European Southern Observatory, 2004.

[2] H. Bonnet, B. Bauvir, A. Wallander, M. Cantzler, J. Carstens, F. Caruso, N. di Lieto, S. Guisard, P. Haguenauer, N. Housen, M. Mornhinweg, J.-L. Nicoud, A. Ramirez, J. Sahlmann, G. Vasisht, S. Wehner, and J. Zagal, "Enabling Fringe Tracking at the VLTI," *The Messenger* **126**, pp. 37–40, Dec. 2006.

[3] R. Stuik, R. Bacon, R. Conzelmann, B. Delabre, E. Fedrigo, N. Hubin, M. Le Louarn, and S. Ströbele, "GALACSI the ground layer adaptive optics system for muse," *New Astronomy Reviews* **49**, pp. 618–624, Jan. 2006.

[4] R. Bacon and others, "The MUSE second-generation VLT instrument," in *Society of Photo-Optical Instrumentation Engineers (SPIE) Conference Series*, *Society of Photo-Optical Instrumentation Engineers (SPIE) Conference Series* **7735**, July 2010.

[5] R. Arsenault and others, "ESO adaptive optics facility," in *Society of Photo-Optical Instrumentation Engineers (SPIE) Conference Series*, *Society of Photo-Optical Instrumentation Engineers (SPIE) Conference Series* **7015**, July 2008.

[6] C. Fuller and A. von Flotow, "Active control of sound and vibration," *IEEE Control Systems* **15**(6), 1995.

[7] L. Sievers and A. von Flotow, "Comparison and extensions of control methods for narrow-band disturbance rejection," *Signal Processing, IEEE Transactions on* **40**(10), 1992.

[8] K. Powell, "Estimating the impact of structural vibration on adaptive optics system performance," *Journal of Applied Optics* **50**, pp. 2185 –2191, May 2011.

[9] J. Veran, C. Irving, A. Beauvillier, and G. Herriot, "Implementation of type-II tip-tilt control in NIFRAOS with woofer-tweeter and vibration cancellation," in *Proc. SPIE 7013, San Diego, USA*, June 2010.

[10] N. Di Lieto, P. Haguenauer, J. Sahlmann, and G. Vasisht, "Adaptive vibration cancellation on large telescopes for stellar interferometry," in *Proc. SPIE 7013, Marseille, France*, June 2008.

[11] S. Meimom, C. Petit, T. Fusco, and C. Kulcsar, "Tip-tilt disturbance model identification for Kalman-based control scheme: application to XAO and ELT systems," *Journal of the Optical Society American A* **27**(11), pp. A122 –A132, 2010.

[12] C. Correia, J. Veran, and G. Herriot, "Advanced vibration suppression algorithms in adaptive optics systems," *Journal of the Optical Society American A* **29**(3), pp. 185 –194, 2010.

[13] E. Fedrigo, R. Donaldson, C. Soenke, R. Myers, S. Goodsell, C. Saunter, and N. Dipper, "SPARTA: Standard Platform for Adaptive optics Real Time Applications," in *Proc. SPIE 6272, Orlando, FL, US*, May 2006.

[14] S. Pigg and M. Bodson, "Adaptive algorithms for the rejection of sinusoidal disturbances acting on unknown plants," *Control Systems Technology, IEEE Transactions on* **18**(4), pp. 822 –836, 2010.

[15] S. Pigg and M. Bodson, "Adaptive harmonic steady-state disturbance rejection with frequency tracking," in *Decision and Control (CDC), 2010 49th IEEE Conference on*, pp. 887–892, IEEE.

[16] S. Kay, *Fundamentals of Signal Processing: Estimation Theory*, vol. 1, Wiley and Sons, Berlin, 2nd ed., 1993.